USHPRR FUEL FABRICATION PILLAR: FABRICATION STATUS, PROCESS OPTIMIZATIONS, AND FUTURE PLANS

J.M. WIGHT
USHPRR Fuel Fabrication Pillar Lead
National Security Directorate, Pacific Northwest National Laboratory
902 Battelle Blvd., Richland WA 99354

V. JOSHI, C.A. LAVENDER
Energy & Environmental Directorate, Pacific Northwest National Laboratory
902 Battelle Blvd., Richland WA 99354

ABSTRACT

The Fuel Fabrication (FF) Pillar, a project within the U.S. High Performance Research Reactor Conversion program of the National Nuclear Security Administration's Office of Material Management and Minimization, is tasked with the scale-up and commercialization of high-density monolithic U-Mo fuel for the conversion of appropriate research reactors to use of low-enriched fuel. The FF Pillar has made significant steps to demonstrate and optimize the baseline co-rolling process using commercial-scale equipment at both the Y-12 National Security Complex (Y-12) and BWX Technologies (BWXT). These demonstrations include the fabrication of the next irradiation experiment, Mini-Plate 1 (MP-1), and casting optimizations at Y-12. The FF Pillar uses a detailed process flow diagram to identify potential gaps in processing knowledge or demonstration, which helps direct the strategic research agenda of the FF Pillar. This paper describes the significant progress made toward understanding the fuel characteristics, and models developed to make informed decisions, increase process yield, and decrease lifecycle waste and costs.

1. Introduction

Low-enriched uranium (LEU) alloyed with 10 wt% molybdenum (U-10Mo) has been identified as a promising alternative to high-enriched uranium (HEU) for the United States High Performance Research Reactors (USHPRR). [1-3] The nominal configuration of the low-enriched U-10Mo plate-type fuel is a metallic U-10Mo fuel foil enriched to slightly less than 20% ^{235}U, the thickness of which varies from 0.6 mm (0.025") to 0.08 mm (0.003") depending on the reactor; a 25 μm thick Zr interlayer–diffusion barrier on either side, and a relatively thick outer cladding of 6061 aluminum. [4, 5] This configuration will require the use of processes and materials not currently in use at the Y-12 National Security Complex (Y-12) and BWX Technologies (BWXT). In order to understand the behavior/characteristics, microstructure development, and challenges associated with fabricating such a fuel, the Fuel Fabrication (FF) Pillar within the National Nuclear Security Administration's Office of Materials Minimization and Management is actively investigating several thermomechanical processing techniques to rapidly determine the most cost-effective and robust method to manufacture the plate fuel and at the same time meet the necessary specifications as required by the reactors/fuel qualifications. [3]

Currently, the baseline model to manufacture U-10Mo alloy consists of multiple complex thermomechanical processes, including casting, homogenization, hot-roll bonding of the Zr diffusion barrier, cold rolling, intermediate annealing, and hot isostatic pressing (HIPing), as

shown in Figure 1. [3] Intermediate cleaning and material handling steps are not described in this figure, but are also actively being pursued, investigated, and implemented as a part of the program at Y-12 and BWXT. The FF Pillar is optimizing this baseline process and actively working toward scaling up the process at these facilities through a series of fabrication campaigns. Some of these fabrication campaigns are integrated with the irradiation tests and characterizations being done at the reactors.

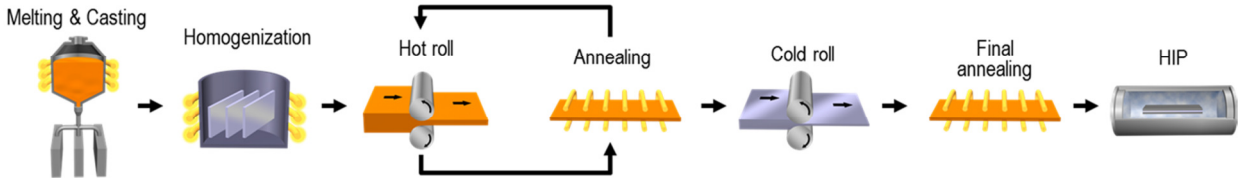

Fig 1. Baseline U-10Mo fuel fabrication steps.

In order to optimize the process and understand the fuel behavior, the FF Pillar works with several national laboratories to support Y-12 and BWXT in optimizing the baseline process. The FF Pillar manages this process through the use of Integrated Product Teams to address the challenges in these major process areas, and other areas as the program deems necessary. Over the years, the labs have systematically investigated the microstructure development and challenges associated with fabrication, and provided solutions to the program. The current paper describes the research conducted and being pursued in these major areas and how it has influenced the fabrication process.

2. Fuel Fabrication Process Optimization

2.1 Casting Optimization

The production of the U-10Mo fuels begins with casting, which is performed at Y-12. This is an important step, and is used to down-blend HEU metal with depleted uranium (DU) to produce LEU and add Mo to make the LEU-Mo alloy. Over the years, the program has actively investigated the effects of feedstock material, the geometry of the molds, the cooling rate, and relevant parameters related to casting. Vacuum induction melting (VIM) was chosen as the casting technique by the program. A casting thickness of 0.2" was selected from existing mold geometries, and in order to maximize productivity, three 0.2" thick plates are produced from each melt.

Initial work by at Y-12 [6] and at Pacific Northwest National Laboratory [7] that investigated the effects of molybdenum feedstock on the impurity content, skull percentage, and uniformity in microstructure demonstrated that a molybdenum rod feedstock provided optimum results. Further development showed that adequate alloying of Mo would require a “master alloy” to reduce melt point mismatch between the U and Mo. A DU-Mo master alloy is now added to the HEU to produce the desired enrichment of 19.75% ^{235}U and Mo content of 10 wt %.

Los Alamos National Laboratory (LANL) and Y-12 have been actively involved in optimizing the design of the VIM casting process. Several critical steps and challenges associated with the mold designs have been addressed. Based on the extensive work performed by these entities, a three-plate mold design (as shown in Figure 1) has been used for the program. Initial efforts with regard to mold design, casting parameters, heat transfer, and modeling of the down-blending were performed in depth by Aiken et al., and recommendations were provided to the program and implemented.

2.2 Homogenization

The U-10Mo as-cast microstructure is an inhomogeneous, dendritic structure with molybdenum-rich and -lean regions (as shown in Figure 2a). [7, 8] It was observed in U-10Mo that, depending on the casting process adopted, microstructures with different grain size, molybdenum inhomogeneity, secondary dendrite arm spacing, and carbide distribution were produced. Mo segregation during casting may affect γ-phase stability and the formation of α phase as well as the phase transition from γ to α and γ′ during thermal processing, such as annealing and HIPing. A homogenization process is needed to reduce Mo segregation and produce desired microstructures with uniformly distributed Mo. The following two sections describe the techniques used by the program to determine the homogenization kinetics and its effect on the phase transformation kinetics and impurities.

2.2.1 Determination of the Homogenization Kinetics

Homogenization of U-10Mo is performed in the γ-phase field (above 560 °C) for several hours. [7-11] The time and temperature required to homogenize is dependent on the grain size and degree of Mo inhomogeneity. Experimentally determining the time and temperature to homogenize is time consuming and labor intensive. In order to overcome this, a homogenization model was developed and is used to reconstruct a Mo concentration map for the entire microstructure domain based on the relationship between a backscattered electron–scanning electron microscope (BSE-SEM) image and energy dispersive spectroscopy (EDS) line data (Figure 2). The homogenization model successfully captures the microstructure information during the homogenization evolution, which is valuable for studying U-10Mo in the subsequent processes and has been described in depth by Xu et al. [12]

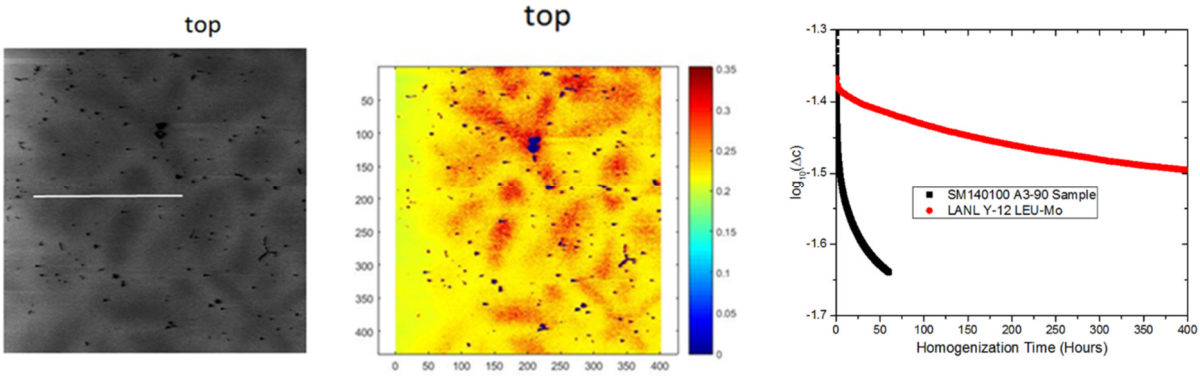

Fig 2. (a) A BSE-SEM image, Mo atomic concentration along the EDS line, and (b) the elemental map reconstruct the Mo concentration for sections of a Y-12 LEU-Mo sample used for MP-1 experiments. (c) Simulated homogenization kinetics for A3-90 [12] and Y-12 LEU-Mo samples.

This modeling work [12] has been applied to provide guidance on the homogenization time required for Y-12 cast MP-1 LEU-10Mo samples. Using EDS analysis performed at LANL, Mo concentration and diffusion distances were determined and then used to determine the homogenization time. The homogenization model based on the BSE-SEM images and EDS line scans, Figure 2a, creates the corresponding Mo map in Figure 2b and then predicts the time required to homogenize the material at 144 h at 900 °C. This modeling approach was used to provide process parameters for the homogenization of the MP1 castings. Thus, the homogenization model not only provides the time and temperature required to homogenize the material for varying casting conditions, but does so more quickly and cost-effectively by

avoiding costly, time-consuming experiments. This modeling tool's mapping capability is also helpful to predict the molybdenum homogeneity in the as-cast and the final formed plates.

2.2.2 Determination of the Impurities and Their Effect on the Phase Transformation Kinetics

In order to fabricate metallic U-10Mo fuel, the as-homogenized ingot is subjected to various rolling and post-rolling steps, such as annealing and HIPing, to form Al-UMo clad fuel. Most of these fabrication steps are carried out between 400 °C and 600 °C. [3] This means a phase transformation of the metastable γ-UMo phase is possible during fabrication steps or during the cooling cycle that might prove deleterious during in-reactor operation. In addition, the alloy chemistry, in particular the presence of minor alloying additions and/or impurity elements in U-Mo alloys, can be another important factor affecting the phase-transformation kinetics. As a part of the program, systematic phase-transformation kinetics was studied in as-cast and homogenized materials during annealing at sub-eutectoid temperatures of 500 °C and 400 °C for the first time, using detailed microstructural characterization techniques such as SEM, X-ray diffraction analysis, scanning transmission electron microscopy (STEM) , and atom probe tomography (APT). [9] Based on the results, we determined that the phase transformation is initiated at both temperatures by cellular transformation, which results in formation of a lamellar microstructure along prior γ-UMo grain boundaries. At 500 °C, cellular transformation is the main mode of transformation (Figure 3a). However, at 400 °C, cellular transformation and precipitation of ordered γ′ U-2Mo phase within the γ-UMo grain interior creates a competitive continuous precipitation situation (Figure 3b). The kinetics of the cellular transformation was found to be very sluggish at 400 °C compared to the kinetics observed at 500 °C, as measured by the transformed area fraction. (Figure 3c)

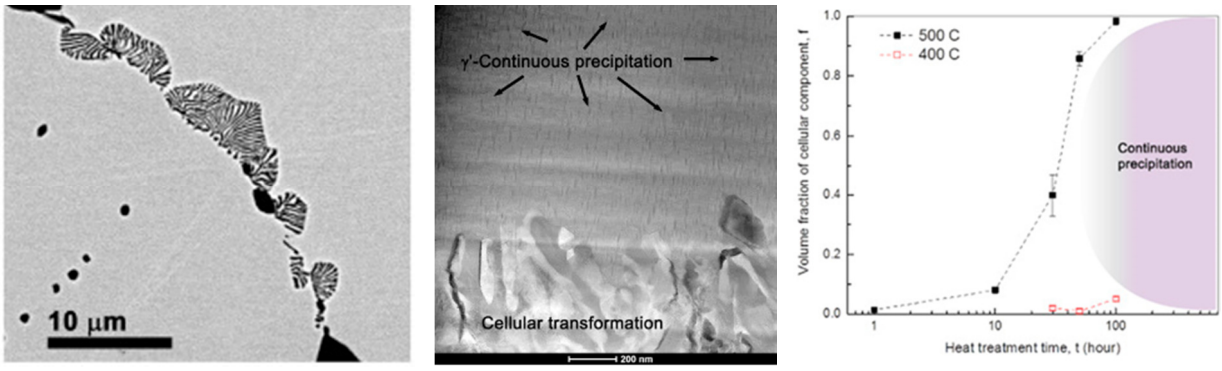

(a) (b) (c)

Fig 3. (a) SEM image of transformed region after 1 h of heat treatment at 500 °C.(b) STEM image of U-Mo sample after heat treatment at 400 °C for 100 h showing uniform continuous precipitation of fine-scale platelike γ′ precipitates inside the γ-UMo matrix. The lamellar cellular transformation product is visible in the bottom half of the image. (c) Volume fraction of phase transformation products vs. time during 500 °C and 400 °C treatment.

Using advanced characterization techniques, we were also able to determine the initiation of discontinuous precipitation from γ-UMo grain boundaries is directly dictated by solute segregation to γ-UMo grain boundaries, forming grain boundary complexions in the homogenized U-10Mo alloy (Figure 4). [13-15] Hence, different homogenization temperatures for the U-10Mo alloy can be used to potentially modify the concentration of impurities dissolved in γ-UMo grain interiors and/or segregated to γ-UMo grain boundaries, and these effects can be used to retard the kinetics of discontinuous precipitation during subsequent sub-eutectoid annealing.

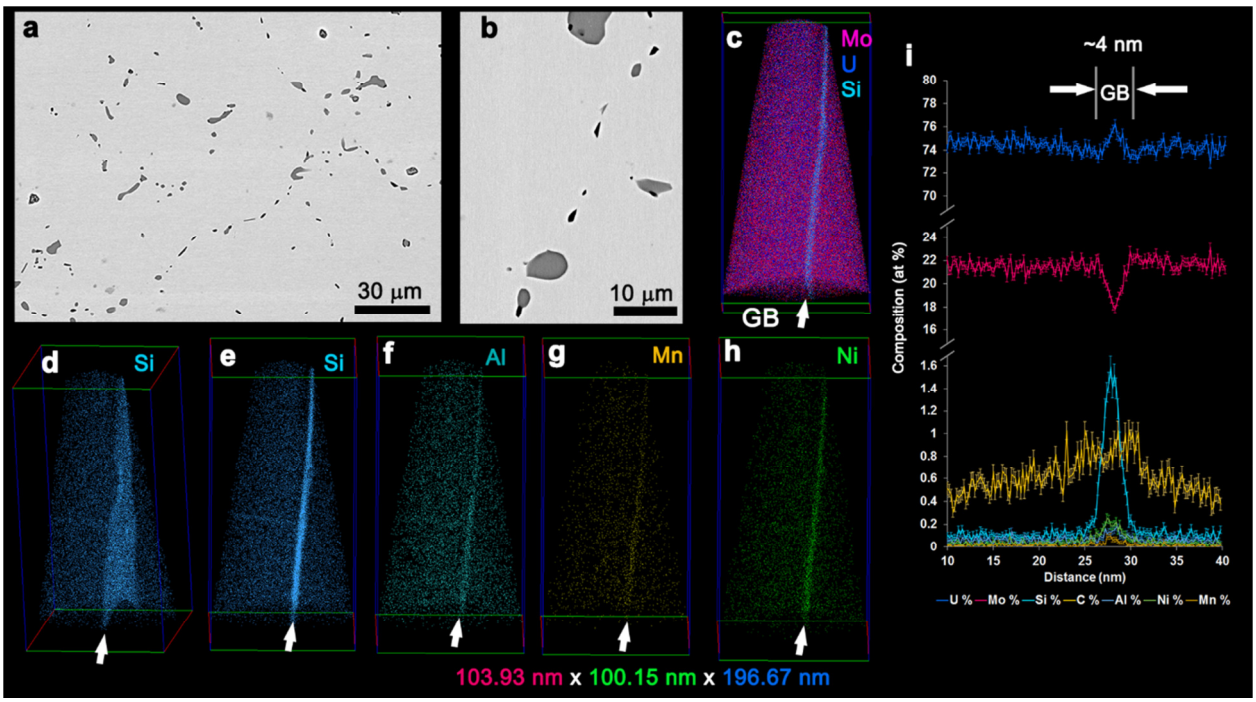

Fig 4. (a) BSE-SEM images of 900 °C-48 hour homogenized U-10Mo alloy microstructure. (b) A higher-magnification image of a specific grain boundary with intermittent presence of uranium carbides (UC) and blocky Si-rich precipitates. (c) γ-UMo grain boundary APT reconstruction showing U (blue), Mo (red), and Si (light blue) at a grain boundary. (d) Si ion map showing clear segregation to grain boundary. (e) A rotated view of the grain boundary plane with Si segregation. Segregation of other elements (f) Al, (g) Mn, and (h) Ni as seen from the ion maps. (i) A quantitative analysis of element segregation at grain boundaries estimated using a 1D concentration profile.

The impurities and phase transformation work have provided in-depth understanding of the phase transformation kinetics and mechanism, and provided the foundation for tailoring the final microstructure after homogenization. In addition, understanding the crystal structure of the impurities has allowed us to provide guidelines to the program regarding techniques to measure the phase transformation in U-10Mo and to accurately determine the density of the alloy. [14, 16-19]

2.3 Rolling Process Development

In order to form the ingots into foils for fuel plate fabrication, the homogenized ingots are rolled in two steps: (1) a hot rolling step to assure bonding of the Zr diffusion barrier and (2) cold rolling to meet dimensional tolerances. Over many years, the Pillar has investigated several different techniques to roll the fuel plate. Several modeling tools [20, 21] have been developed and used to predict the mill parameters, defects, Zr clad variation during rolling, microstructure effects, optimization of the rolling schedule, and improving the yield of the process. The following sections describe the important tools/models used by the program to address these.

2.3.1 Simulation of Rolling Process (Macro Approach)

The commercial finite-element modeling code LS-Dyna was used to develop a macroscopic model to simulate hot and cold multi-pass rolling. A model developed by Soulami et al. [20] was first validated through comparison with actual rolling data, and then used to perform various parametric studies investigating the effect of can material on the rolled sheet defects, effect of roll diameters and coupon geometries on the roll separating forces, etc. This modeling tool can be used by fuel manufacturers to design their rolling schedules and select

the appropriate equipment. Figure 5a shows a comparison between measured roll separation force and model predictions.

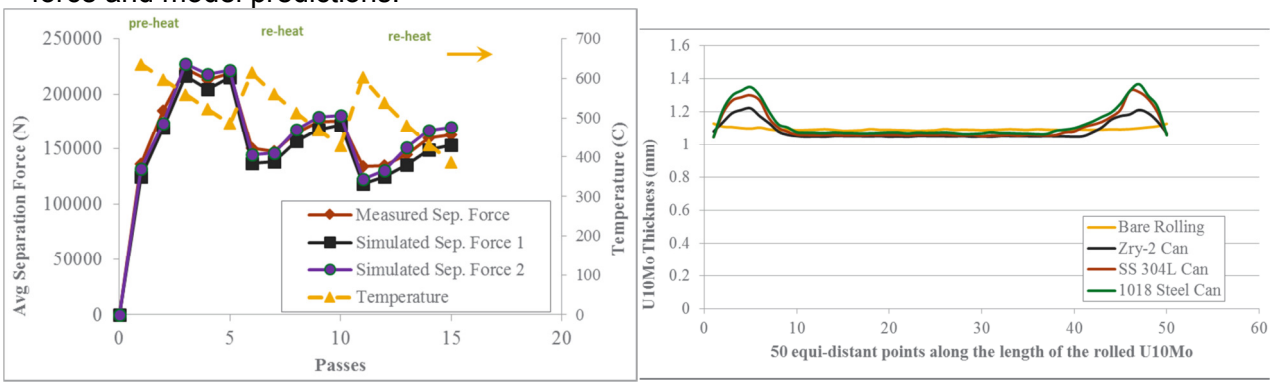

(a) (b)

Fig 5. (a) Measured and modeled load separation force used to determine the mill parameters. (b) Effect of canning material on dog-boning defects during U-10Mo rolling.

The model was also used to predict rolling defects due to can material. Four cases were considered in this parametric study: (1) rolling of a U-10Mo coupon inside a 1018 steel can, (2) rolling of a U-10Mo coupon inside a 304 stainless steel can, (3) rolling of a U-10Mo coupon inside a Zircaloy-2 can, and (4) bare rolling of a U-10Mo coupon. To quantify the observed dog-boning in the simulations, the thickness variation along the centerline of the U-10Mo sheet was plotted, as shown in Figure 5b. The bare rolling case does not show any dog-boning, and the thickness is relatively uniform along the coupon. Dog-boning amplitude is inversely proportional to the strength of the can material. In fact, the stronger the can material, the less likely localized thickening of the fuel alloy and thinning of the cladding at the edges of the fuel core will occur.

2.3.2 Microstructure Development during Rolling Process

As-cast and homogenized U-10Mo typically contains second-phase particles, such as UC and silicides, along the grain boundaries. The volume fraction of UC is typically large, while the other phases can be redissolved in the matrix by certain heat treatments. The UC particle distribution is important because of its influence on the recrystallization processes (particle stimulated nucleation) that occur during annealing between rolling passes. Unfavorable particle distribution and fracture after rolling can affect the grain size and also influence the in-reactor fuel performance. [22] This study was used primarily to provide guidelines on the desired microstructure required upon casting/homogenization.

The effect of second-phase particles i.e., particle volume fraction (PVF), particle size, and their distribution and morphology, on the formation of stringers in hot-rolled alloys and their eventual effect on grain structures after recrystallization have been investigated and quantified. Figure 6a shows microstructure of as-cast and homogenized samples that had different distributions, sizes, and volume fractions of second-phase particles. The multi-pass hot-rolling process of a U-10Mo coupon was studied by plane-strain compression finite-element modeling. [21] Depending on the morphology, size, and shape of the particles and the stringers, the formation of stringers results in reduced strength of the final formed fuel and induces a network of small grains to develop across the cross section, which may be detrimental to the fuel performance. Quantitative techniques to measure the PVF and stringer volume fraction (SVF) have been developed. The results have been verified experimentally to accurately predict the microstructure of the final formed fuel and have been documented by Hu et al. [21]. In order to predict the grain structure, recovery and recrystallization studies were performed, and the activation energy was calculated. Potts modeling was introduced to predict the microstructure after annealing (Figure 7). The SVF for individual samples that had randomly distributed, circular particles was almost unchanged by hot rolling reduction.

However, the SVF increased significantly in the same process for a sample that had high-aspect-ratio particles distributed along the grain boundaries. PVF and SVF have significant effects on the final microstructure: the average grain size is smaller with a higher PVF, and the deviation of grain size after recrystallization is higher with a higher SVF. This study supports processing parameter optimization and materials selection for metallic materials that include second-phase particles. The stringer analyses show that the SVF will increase with rolling reduction when the particles are distributed along grain boundaries. The high-aspect-ratio particles distributed along grain boundaries will increase the SVF rapidly with rolling reduction. However, randomly distributed particles are less likely to form stringers during rolling reduction. The heterogeneity of grain size distribution, or the grain size deviation, after recrystallization is strongly related to the SVF in the microstructure: the higher the SVF, the larger the grain size deviation.

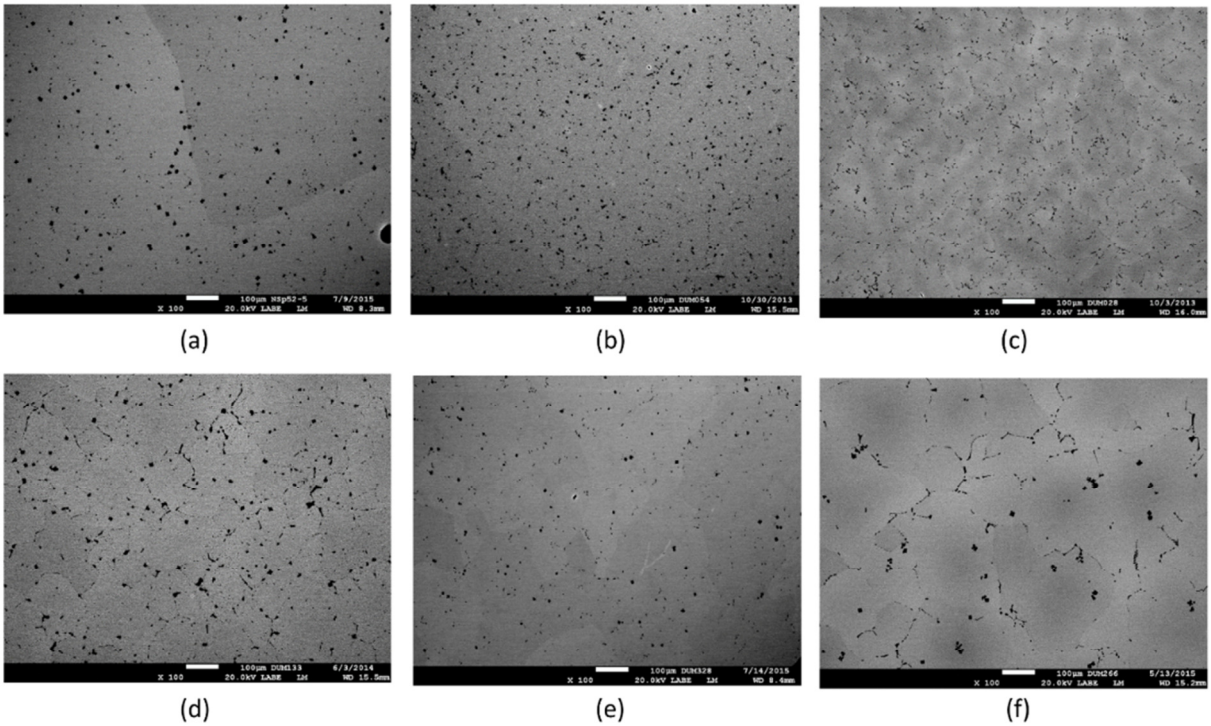

Fig 6. SEM images of initial microstructures for six samples: (a) sample-1, (b) sample-2, (c) sample-3, (d) sample-4, (e) sample-5, and (f) sample-6. (The solid black particles are carbides and the gray areas are U-10Mo matrix).

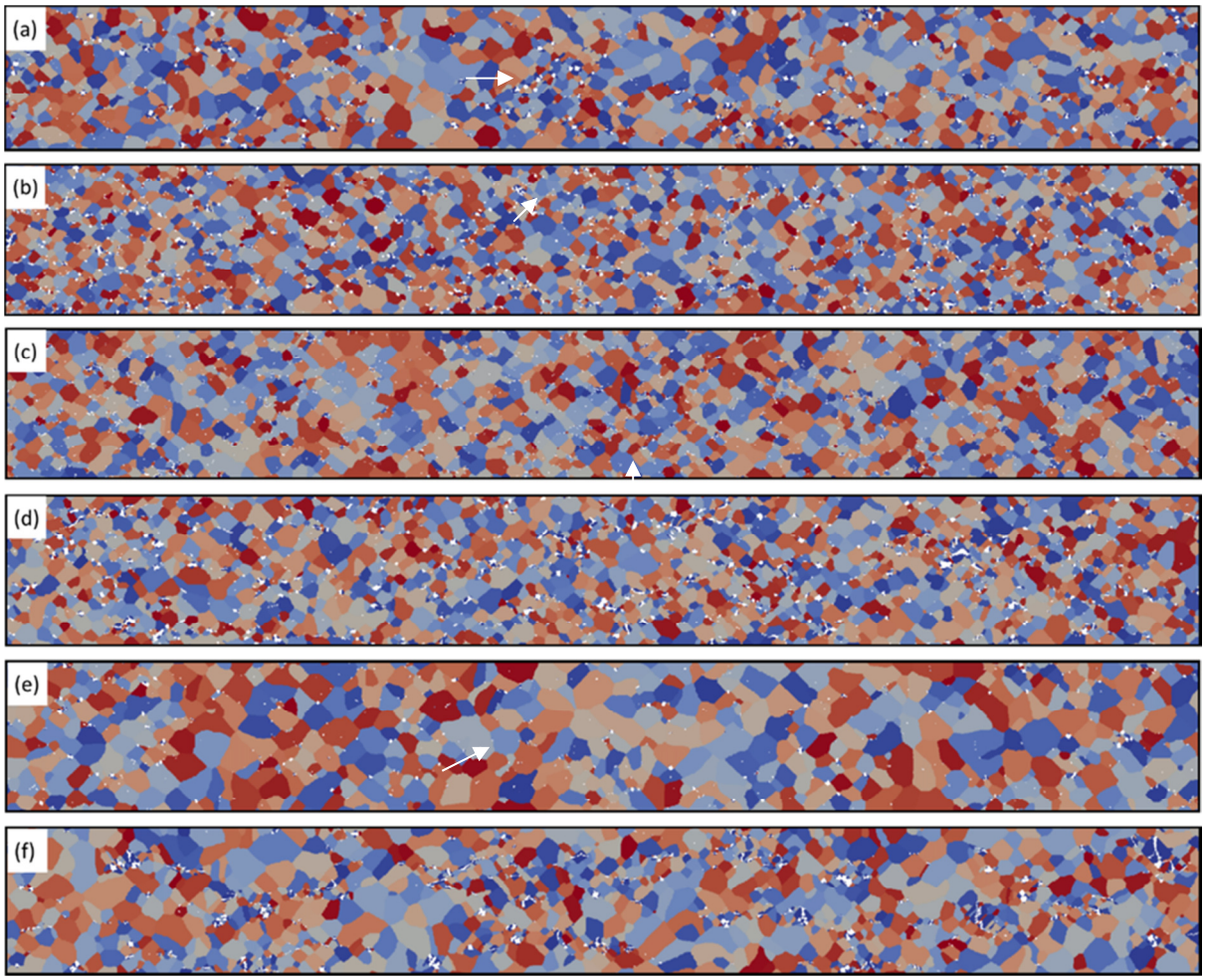

Figure 7. The recrystallized microstructures predicted by the Potts model after 60% rolling reduction and annealing of the six U-10Mo samples shown in Figure 6: (a) sample-1, (b) sample-2, (c) sample-3, (d) sample-4, (e) sample-5, and (f) sample-6. White arrows show the non-uniform/ smaller grain size as compared to matrix grain size.

2.3.3 Effect of Annealing on Grain Growth and Phase Transformation Kinetics

Annealing is performed as a final stage to relieve the stresses after cold rolling and flatten the foils prior to loading into the HIP can. Additionally, the final grain size/distribution of the foil developed during annealing affects the amount of phase transformation during the subsequent HIP cycle, and potentially the in-reactor fuel performance.

Systematic experiments [22] and the Potts model were used to determine the grain growth kinetics and simulate U-10Mo grain growth, respectively (Figure 8). Temperature-dependent stagnation behavior caused by the presence of second-phase particles at temperatures of 700 °C–900 °C was accounted for by modifying the nonphysical Potts model temperature. BSE-SEM micrographs of as-rolled and annealed U-10Mo were used to construct initial simulation microstructures. Average grain sizes and grain size distributions obtained through Potts model simulations were found to be in reasonable agreement with experimental observations. Repeating the simulations for a synthetically generated dispersion of particles yielded similar results with slightly slower grain growth. Departure from theoretical Zener pinning (Figure 8b) behavior in the simulations was shown to occur because grain boundary fluctuations occurred on the same length scale as the second-phase particles.

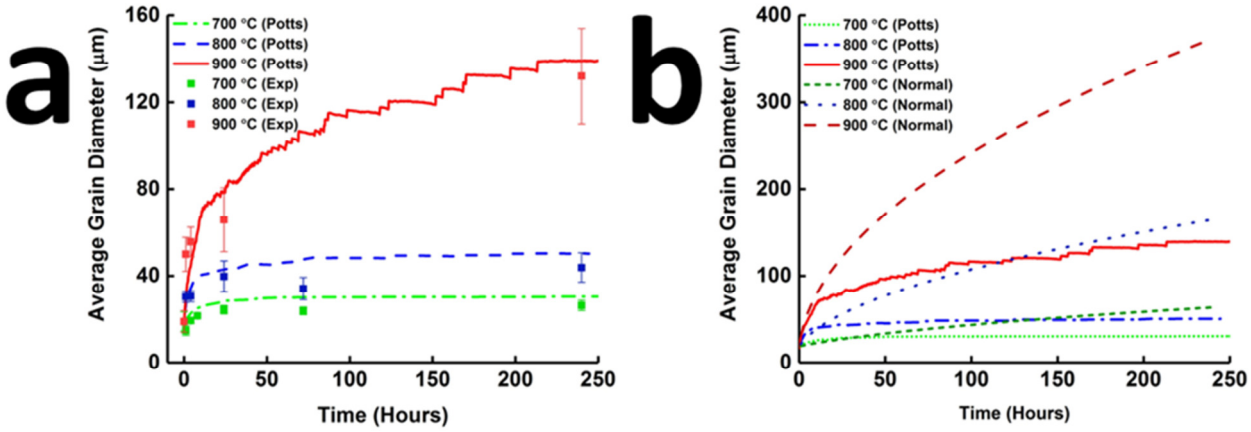

Fig 8. The average grain size of U-10Mo as predicted by the Potts model, assuming an activation energy for grain growth of 172.4 kJ/mole, compared with the experimentally obtained grain growth data (a) and the behavior predicted for normal grain growth (b).

The effect of sub-eutectoid heat treatment on the phase transformation behavior in rolled U-10Mo foils was systematically investigated. [23] Three starting microstructures were evaluated; all were initially hot and cold rolled to 0.2 mm (as-rolled condition): (1) as-rolled, (2) as-rolled + annealed at 700 °C for 1 h, and (3) as-rolled + annealed at 1000 °C for 60 h. Annealing of as-rolled materials at 700 °C resulted in small grains (15 ± 9 μm average grain size), while annealing at 1000 °C led to very large grains (156 ± 118 μm average grain size) in rolled U-10Mo foils. Later, the samples were subjected to sub-eutectoid heat-treatment temperatures of 400 °C, 500 °C, and 550 °C for different durations from 1 h to 100 h. U-10Mo rolled foils underwent various degrees of decomposition when subjected to the sub-eutectoid heat treatment, and formed a lamellar microstructure through a cellular reaction mostly along the previous γ-UMo grain boundaries. The smallest amount of cellular reaction occurred in the large-grain microstructure at all temperatures. Conversely, a substantial amount of cellular reaction occurred in both the as-rolled and the small-grained microstructure. After 100 h of heat treatment at 500 °C, the volume fractions of the lamellar phase were 4%, 22%, and 82% in large-grain, as-rolled, and small-grain samples, respectively.

3. Conclusions

This paper described the significant progress made toward understanding the fuel characteristics, and models developed to make informed decisions, increase process yield, and decrease lifecycle waste and costs. Modeling and characterization efforts are producing actionable information that is being integrated to optimize the fuel fabrication baseline. This work supports resolution of technical gaps, development of process specifications, and production planning. Modeling efforts enable the program to understand the effects of feedstock and process variabilities (operating windows). We are providing reusable tools that will guide subsequent experiment, demonstration, and conversion activities. Results are communicated to stakeholders through reports, journal articles, and technical bulletins.

4. References

[1] M.K. Meyer, G.L. Hofman, S.L. Hayes, C.R. Clark, T.C. Wiencek, J.L. Snelgrove, R.V. Strain, K.H. Kim, Low-temperature irradiation behavior of uranium–molybdenum alloy dispersion fuel, Journal of Nuclear Materials 304(2-3) (2002) 221-236.
[2] H. Ozaltun, M.H.H. Shen, P. Medvedev, Assessment of residual stresses on U10Mo alloy based monolithic mini-plates during Hot Isostatic Pressing, Journal of Nuclear Materials 419(1-3) (2011) 76-84.
[3] D.J. Senor, D.E. Burkes, Fuel Fabrication Capability Research and Development Plan, PNNL-22528, Pacific Northwest National Laboratory, Richland, Washington, 2014.

[4] Low Enriched Uranium Monolithic Fuel Plates: Functional and Operational Requirements, Idaho National Laboratory, Idaho Falls, Idaho 2014.
[5] GTRI: Reducing Nuclear Threats, 2014.
[6] A.L. DeMint, J.G. Gooch, K.R. Crane, D.E. Fleury, Uranium-10% Molybdenum Parametric Study 1: Alloying, Y-12 National Security Complex, Oak Ridge, Tennessee, 2013.
[7] E.A. Nyberg, V.V. Joshi, C.A. Lavender, D.M. Paxton, D.E. Burkes, The Influence of Casting Conditions on the Microstructure of As-Cast U-10Mo Alloys: Characterization of the Casting Process Baseline, Pacific Northwest National Laboratory, Richland, Washington, 2013.
[8] E.A. Nyberg, V.V. Joshi, C.A. Lavender, D.M. Paxton, D.E. Burkes, Influence of Homogenization on the Mechanical Properties and Microstructure of the U-10Mo Alloy, PNNL-23348, Pacific Northwest National Laboratory, Richland, Washington, 2014.
[9] S. Jana, A. Devaraj, L. Kovarik, B. Arey, L. Sweet, T. Varga, C. Lavender, V. Joshi, Kinetics of cellular transformation and competing precipitation mechanisms during sub-eutectoid annealing of U10Mo alloys, Journal of Alloys and Compounds 723 (2017) 757-771.
[10] V.V. Joshi, C. Lavender, Z. Xu, D. Paxton, D. Burkes, The effect of grain size on the homogenization kinetics and eutectoid decomposition in U-10 wt% Mo alloys, TMS 2016 145th Annual Meeting and Exhibition, Nashville, Tennessee, 2016.
[11] V.V. Joshi, E.A. Nyberg, C.A. Lavender, D. Paxton, D.E. Burkes, Thermomechanical process optimization of U-10wt% Mo – Part 2: The effect of homogenization on the mechanical properties and microstructure, Journal of Nuclear Materials 465 (2015) 710-718.
[12] Z. Xu, V. Joshi, S. Hu, D. Paxton, C. Lavender, D. Burkes, Modeling the homogenization kinetics of as-cast U-10wt% Mo alloys, Journal of Nuclear Materials 471 (2016) 154-164.
[13] A. Devaraj, L. Kovarik, E. Kautz, B. Arey, S. Jana, C. Lavender, V.V. Joshi, submitted Acta Materialia.
[14] A. Devaraj, L. Kovarik, V.V. Joshi, S. Jana, S. Manandhar, B.W. Arey, C.A. Lavender, High-Resolution Characterization of UMo Alloy Microstructure, PNNL-26020, Pacific Northwest National Laboratory, Richland, Washington, 2016.
[15] A. Devaraj, R. Prabhakaran, V.V. Joshi, S.Y. Hu, E. McGarrah, C.A. Lavender, Theoretical Model for Volume Fraction of UC, 235U Enrichment, and Effective Density of Final U 10Mo Alloy, PNNL-SA-117284, Pacific Northwest National Laboratory, 2016.
[16] A. Devaraj, S. Jana, C.A. McInnis, N.J. Lombardo, V.V. Joshi, L.E. Sweet, S. Manandhar, C.A. Lavender, Detecting the Extent of Eutectoid Transformation in U-10Mo, PNNL-SA-120714, Pacific Northwest National Laboratory (PNNL), Richland, WA (US), 2016.
[17] E.J. Kautz, A. Devaraj, L. Kovarik, C.A. Lavender, V.V. Joshi, Effect of Silicon in U-10Mo Alloy, PNNL-26790, Pacific Northwest National Laboratory, Richland, WA (United States), 2017.
[18] E.J. Kautz, S. Jana, A. Devaraj, C.A. Lavender, L.E. Sweet, V.V. Joshi, Detecting the Extent of Cellular Decomposition after Sub-Eutectoid Annealing in Rolled UMo Foils, PNNL-26862, Pacific Northwest National Laboratory, Richland, WA (United States), 2017.
[19] R. Prabhakaran, A. Devaraj, V.V. Joshi, C.A. Lavender, Procedure for Uranium-Molybdenum Density Measurements and Porosity Determination, PNNL-25793, Pacific Northwest National Laboratory, Richland, WA (United States), 2016.
[20] A. Soulami, D.E. Burkes, V.V. Joshi, C.A. Lavender, D. Paxton, Finite-element model to predict roll-separation force and defects during rolling of U-10Mo alloys, Journal of Nuclear Materials 494 (2017) 182-191.
[21] X. Hu, X. Wang, V.V. Joshi, C.A. Lavender, The effect of thermomechanical processing on second phase particle redistribution in U-10 wt%Mo, Journal of Nuclear Materials 500 (2018) 270-279.
[22] W.E. Frazier, S. Hu, N. Overman, C. Lavender, V.V. Joshi, Short communication on Kinetics of grain growth and particle pinning in U-10 wt.% Mo, Journal of Nuclear Materials 498 (2018) 254-258.
[23] S. Jana, N. Overman, T. Varga, C. Lavender, V.V. Joshi, Phase transformation kinetics in rolled U-10 wt. % Mo foil: Effect of post-rolling heat treatment and prior γ-UMo grain size, Journal of Nuclear Materials 496 (2017) 215-226.